Mutational Analysis of C-Lobe Ligands of Human Serum Transferrin: Insights into the Mechanism of Iron Release†

Anne B. Mason,*,‡ Peter J. Halbrooks,‡ Nicholas G. James,‡ Susan A. Connolly,‡ Julia R. Larouche,‡ Valerie C. Smith,§ Ross T. A. MacGillivray,§ and N. Dennis Chasteen||

Department of Biochemistry, University of Vermont College of Medicine, Burlington, Vermont 05405-0068, Department of Biochemistry and Molecular Biology, University of British Columbia, Vancouver, British Columbia V6T 1Z3, Canada, and Department of Chemistry, Parsons Hall, University of New Hampshire, Durham, New Hampshire 03824

Received January 4, 2005; Revised Manuscript Received March 16, 2005

ABSTRACT: Each homologous lobe of human serum transferrin (hTF) has one Fe^{3+} ion bound by an aspartic acid, a histidine, two tyrosine residues, and two oxygens from the synergistic anion, carbonate. Extensive characterization of these ligands in the N-terminal lobe has been carried out. Despite sharing the same set of ligands, there is a substantial amount of evidence that the N- and C-lobes are inequivalent. Studies of full-length hTF have shown that iron release from each lobe is kinetically distinguishable. To simplify the assessment of mutations in the C-lobe, we have created mutant hTF molecules in which the N-lobe binds iron with high affinity or not at all. Mutations targeting the C-lobe liganding residues have been introduced into these hTF constructs. UV−visible spectral, kinetic, and EPR studies have been undertaken to assess the effects of each mutation and to allow direct comparison to the N-lobe. As found for the N-lobe, the presence of Y517 in the C-lobe (equivalent to Y188 in the N-lobe) is absolutely essential for the binding of iron. Unlike the N-lobe, however, mutation of Y426 (equivalent to Y95) does not produce a stable complex with iron. For the mutants that retain the ability to bind iron (D392S and H585A), the rates of release are considerably slower than those measured for equivalent mutations in the N-lobe at both pH 7.4 and pH 5.6. Equilibrium binding experiments with HeLa S_3 cells indicate that recombinant hTF, in which Y426 or H585 is mutated, favor a closed or nearly closed conformation while those with mutations of the D392 or Y517 ligands appear to promote an open conformation. The differences in the effects of mutating the liganding residues in the two lobes and the subtle indications of cooperativity between lobes point to the importance of the transferrin receptor in effecting iron release from the C-lobe. Significantly, the equilibrium binding experiments also indicate that, regardless of which lobe contains the iron, the free energy of binding is equivalent and not additive; each monoferric hTF has a free energy of binding that is 82% of diferric hTF.

Human serum transferrin (hTF)[1] is comprised of two homologous lobes, termed the N- and C-lobes, each of which binds a single atom of iron in a deep cleft defined by two subdomains (termed N-I and N-II and C-I and C-II domains, respectively) (*1*, *2*). As in most transferrins, the amino acid residues responsible for the specific and tight binding of iron in the C-lobe of hTF are an aspartic acid at position 392 (the sole ligand from the C-I domain), a tyrosine at position 426 which lies in the hinge at the edge of the C-II domain, a second tyrosine at position 517 in the C-II domain, and a histidine residue at position 585 in the hinge bordering the C-I domain. In addition, the iron atom is coordinated by two oxygen atoms from the synergistic carbonate anion. In turn, the carbonate is itself stabilized by a hydrogen bond from a conserved arginine residue at position 456 (residing in the C-II domain) (Figure 1). Further stabilization of the carbonate is provided by a conserved threonine residue and a main chain amide at the end of α-helix 5. Structural information on the iron-containing hTF C-lobe is currently limited to a crystal structure at 3.3 Å resolution (*3*), although structures of the closely related pig (2.15 Å) and rabbit transferrins (2.6 Å) are available (*4*).

The function of hTF in the plasma is to bind iron and to deliver it to cells bearing the specific transferrin receptor 1

† This work was supported by USPHS Grants R01 DK 21739 (A.B.M.) and R01 GM 20194 (N.D.C.) and a NRSA Thrombosis and Hemostasis Postdoctoral Fellowship (S.A.C.).

* Correspondence should be addressed to this author: e-mail, anne.mason@uvm.edu; phone, (802) 656-0343; fax, (802) 862-8229.

‡ University of Vermont College of Medicine.

§ University of British Columbia.

|| University of New Hampshire.

[1] Abbreviations: hTF, human serum transferrin; hTF/2N, the N-lobe of human serum transferrin; N-His hTF-NG, recombinant nonglycosylated human serum transferrin with a factor Xa cleavage site and a hexa-His tag attached to the amino terminus of the protein; N-His Y95F/Y188F hTF-NG, monoferric hTF with iron in the C-lobe; N-His Y426F/Y517F hTF-NG, monoferric hTF with iron in the N-lobe; N-His Y95F/Y188F/Y426F/Y517F hTF-NG, apo-hTF; oTF, ovotransferrin; TFR, transferrin receptor 1; DMEM-F12, Dulbecco's modified Eagle's medium−Ham F-12 nutrient mixture; BHK cells, baby hamster kidney cells; UG, Ultroser G; FBS, fetal bovine serum; BSA, bovine serum albumin; HRP, horseradish peroxidase; TMB, 3,3′,5,5′-tetramethylbenzidine; BA, butyric acid; Tiron, 4,5-dihydroxy-1,3-benzenedisulfonic acid; EDTA, ethylenediaminetetraacetic acid; HEPES, *N*-(2-hydroxyethyl)piperazine-*N*′-2-ethanesulfonic acid; MES, morpholinoethanesulfonic acid; Ni-NTA, nickel nitrilotriacetic acid; EPR, electron paramagnetic resonance.

10.1021/bi050015f CCC: $30.25
Published on Web 05/12/2005

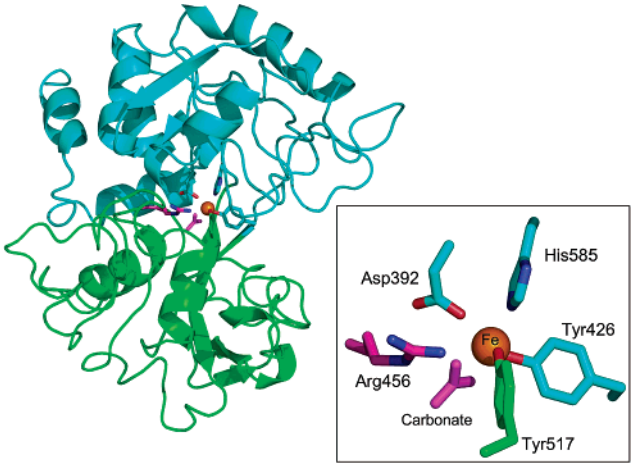

FIGURE 1: Ribbon diagram of the C-lobe of hTF [from the Zuccola structure (*3*)] showing the location of the liganding residues. The C-I domain is depicted in cyan and the C-II in green. The inset provides a close-up view of the liganding residues D392, Y426, Y517, and H585 as well as the R456 (magenta) residue that stabilizes binding of the synergistic anion, carbonate (magenta). The figure was created using PyMOL (*49*).

(TFR) by the process of receptor-mediated endocytosis (*5*). The details of the molecular mechanism(s) responsible for the ability of the individual lobes of hTF to bind and release iron are being actively addressed (*6*, *7*). The structures of both the iron-bound and apo conformation of the N-lobe (hTF/2N) have been solved, providing snapshots of the N-lobe at the beginning and end of the iron ligation cycle (*8*, *9*). As revealed by these two structures, a large conformational change accompanies iron binding and release. Analysis of the N-lobe liganding residues, (D63, Y95, Y188, and H249) via site-directed mutagenesis has contributed to a model of how these residues composing the iron binding site function in the reversible binding and release of iron. Important conclusions from this work include the fact that Y188 is required for iron binding (*10*). In addition, the H249A mutant leads to a greater destabilization of iron binding than either the D63S or Y95F mutants at both pH 7.4 and pH 5.6, as reflected by their faster rates of iron release; the difference is greater at the higher pH. In addition, the dilysine trigger (composed of K206 and K296 which probably share a hydrogen bond in the iron form of the N-lobe) has been identified as a critical feature for controlling iron release in a pH-dependent manner. In particular, substitution of glutamic acid for the lysine at position 206 results in an extremely slow rate of iron release from the N-lobe (especially at the putative endosomal pH of 5.6) which is attributed to salt bridge formation between the glutamic acid and lysine residues (*7*).

While these studies have increased our understanding of how the N-lobe functions, similar approaches to study the C-lobe have been largely unsuccessful. Efforts to express the isolated recombinant C-lobe have yielded only modest amounts of protein (*11*), requiring that other strategies be utilized to obtain the functional C-lobe. For example, insertion of a factor Xa cleavage site in the hinge between the two lobes of full-length hTF has led to generation of the C-lobe by proteolysis of the full-length construct (*12*). In the current study a different approach has been taken. Previously, we produced full-length hTF with an N-terminal hexa-His tag containing mutations which control the ability of the N-lobe to bind iron tightly (K206E) or not at all (Y95F/Y188F) (*13*). In that work, we clearly documented the lack of effect of the His tag on any measurable function; this finding was recently confirmed in a mass spectrometry study (*14*). Also, the rate of release of iron from the C-lobe was shown to be identical (within experimental error) in the presence and absence of the K206E mutation (*13*). These studies further substantiated much previous work demonstrating that the N- and C-lobes of hTF differ in a number of properties (*15*−*19*). For example, it is clear that the effects of temperature and pH on the release rates from each lobe differ and that release of iron from the C-lobe is sensitive to salt concentration in a linear manner at both pH 7.4 and pH 5.6. In contrast, the presence of salt at pH 7.4 actually slows iron release from the N-lobe; a crossover point occurs at pH ~6.2 below which salt exerts the opposite effect and accelerates iron release (*7*).

In the present work, each of the C-lobe iron liganding residues in full-length hTF with modified N-lobes has been mutated to mimic the substitutions that were made in the N-lobe of hTF. UV−vis and EPR analyses as well as kinetic observation of iron release by each protein at pH 5.6 and 7.4 have been carried out. Estimates of binding affinities to TF receptors on HeLa S_3 cells provide additional information on the ability of the C-lobe mutants to bind metal and undergo the conformational change ordinarily resulting from such binding. The work provides a basis for comparisons of the individual ligands in each lobe and some explanation for the well-documented differences in the binding and release properties of the two lobes.

MATERIALS AND METHODS

Materials. Dulbecco's modified Eagle's medium−Ham F-12 nutrient mixture (DMEM-F12), and antibiotic−antimycotic solution (100×) were from Gibco-BRL Life Technologies. Fetal bovine serum (FBS) was obtained from Atlanta Biologicals (Norcross, GA) and was tested prior to use to ensure adequate growth of BHK cells. Ultroser G (UG) is a serum replacement from BioSepra (Cergy, France). Bovine factor Xa was purchased from Haematologic Technologies, Inc. (Essex Junction, VT). The Quik-change mutagenesis kit was from Stratagene. Ni-NTA resin came from Qiagen. Corning expanded surface roller bottles and Dynatech Immunolon 4 Removawells were obtained from Fisher Scientific. The chromatographic resin, Poros 50 HQ, was from Applied Biosystems. A Hi-Prep 26/60 Sephacryl S-200HR column was from Amersham Pharmacia. Methotrexate from Bedford Laboratories was purchased at a local hospital pharmacy and used for selection of plasmid-containing cells. Centricon 30 microconcentrators, YM-30 ultrafiltration membranes, and a spiral cartridge concentrator (CH2PRS) fitted with an S1Y10 cartridge were from Millipore/Amicon. Bovine serum albumin (BSA) was from Sigma. Rabbit anti-mouse immunoglobulin G was from Southern Biological Associates. Immunopure NHS-LC-biotin and immunopure avidin−horseradish peroxidase were from Pierce, as was the INDIA His probe HRP. The TMB Microwell peroxidase substrate system was obtained from Kirkegaard and Perry Laboratories (Gaithersburg, MD). All other chemicals and reagents were of analytical grade.

Preparation of Plasmids. The Quik-change protocol from Stratagene was used to introduce mutations into the hTF

cDNA in the pNUT vector as described previously (*20*). All of the hTF constructs lacked the N-linked glycosylation sites and contained an N-terminal hexa-His tag (*13*, *21*). Two complementary mutagenic primers were designed for each of the C-lobe liganding residues: D392, Y426, Y517, and H585. Both the amino acid change and the mutated nucleotides are shown in bold (only the coding strand primers are shown) (*22*): D392**S**, 5′-GATGCCATGAGCTTG**TC**TGGAGGGTTTGTCTACATAGCG-3′; Y426**F**, 5′-CCAGAGGCAGGGT**T**TTTCGCTGTAGCAGTGG-3′; Y517**F**, 5′-AAAGAGGGATACTACGGCT**T**CACAGGCGCTTTCAGG-3′; H585**A**, 5′-AGAGCCCCGAAT**GC**CGCTGTGGTCACACGG-3′.

The mutations were introduced into full-length hTF containing either (1) a K206E mutation or (2) a Y95F/Y188F double mutant. As indicated above, the first construct leads to a protein in which iron is held very tightly in the N-lobe and the second to a construct lacking the ability to bind iron in the N-lobe at all. Production of control constructs N-His Y426F/Y517F hTF-NG (monoferric N-lobe) and N-His Y95F/Y188F/Y426F/Y517F hTF-NG (apo-hTF) has been described in detail elsewhere (*22*). The complete nucleotide sequences of all clones were determined prior to transfection of the plasmid into BHK cells.

Protein Expression and Purification. Expression and purification of the recombinant hTFs were carried out as previously described (*22*). Briefly, the recombinant protein is secreted from BHK cells into the surrounding tissue culture medium. The recombinant hTF is then isolated from the media by a series of chromatographic steps including Poros 50 HQ, Qiagen Ni-NTA, and Sephacryl S200HR columns to yield a single band on Coomassie blue stained SDS−PAGE gels. As described, more recently, the Poros 50 HQ column was eliminated from the protocol (*22*). The hTF is recovered from the S200HR column in 100 mM NH_4HCO_3, reduced in volume to 15 mg/mL, and stored at −20 °C until use. The yield of hTF prior to the final step is determined by a competitive immunoassay (*23*). Following the gel filtration column the concentration is determined by spectral analysis using the previously reported extinction coefficients (*22*).

Removal of the Hexa-His Tag. Tagged proteins were exchanged into 50 mM Tris-HCl, pH 8.0, containing 100 mM NaCl and 5 mM $CaCl_2$ using a Centricon 30 microconcentrator. The His tag was removed by bovine factor Xa at a ratio of 1 μg/50 μg of hTF in a total sample volume of ∼1.3 mL in an Eppendorf tube rotated at room temperature for 48 h. Aliquots were removed at timed intervals and frozen prior to electrophoresis on a 10% SDS−PAGE gel. The extent of the cleavage was monitored by blotting with INDIA His probe HRP according to the instructions from Pierce. Following cleavage, each sample was exchanged in Centricon microconcentrators into buffer for passage over a 10 mL column of Qiagen Ni-NTA. The flow-through from that column (lacking the His tag) was concentrated, and final purification was achieved on a S200HR column in 100 mM NH_4HCO_3. The cleavage of the His tag yields the "native" hTF sequence (residues 1−679) lacking carbohydrate.

Spectral Analysis. A full absorbance spectrum for each iron-loaded hTF was collected in the presence of 100 mM HEPES, pH 7.4, at 25 °C using a Varian CARY-100 spectrophotometer. Difference spectra were obtained following subtraction of the buffer absorbance over the range of wavelengths from 500 to 250 nm.

Iron Removal Protocol. Our standard protocol was used to remove iron from the recombinant hTF. Briefly, each sample was placed into a Centricon 30 microconcentrator and treated with 0.5 M sodium acetate, pH 4.9, containing 1 mM NTA and 1 mM EDTA until all color disappeared. The sample was then sequentially exchanged in the Centricon with 2 mL additions of 100 mM KCl, 100 mM sodium perchlorate, 100 mM KCl (× 3), and finally 100 mM NH_4HCO_3 (× 5). Following each 2 mL addition, the sample was reduced to <100 μL in the microconcentrators.

EPR Spectra. Frozen solution EPR spectra of iron hTF were obtained at 77 K on a Bruker ElexSys X-band (9.1−9.8 GHz) EPR spectrometer. Calibrated quartz sample tubes of 3 mm i.d. and 4 mm o.d. were employed with a liquid N_2 dewar inserted into the high-sensitivity HSQ cavity. Typical spectrometer settings for iron(III)−hTF samples were microwave frequency = 9.162 GHz, microwave power = 20 mW, modulation amplitude = 10 G, scan range = 1800 G, scan time = 83.89−671.09 s with a time constant = 0.1638−1.310 s, and number of scans = 1−20 depending on the sample.

Kinetics of Iron Release. As described in detail elsewhere, the rate of iron release from the C-lobe of recombinant hTF was determined using a CARY-100 spectrophotometer (*20*). In the previous work, the temperature was maintained at 37 °C due to the slow iron release rates from the particular mutants under study. In the present study, experiments were performed at 25 °C to slow the release rates and also to allow direct comparisons to the N-lobe liganding mutants. Even at 25 °C the rates of release for the liganding mutants were too fast to measure on the CARY-100. Instead, either absorbance or fluorescence data were collected using an OLIS-RSM-1000 stopped-flow spectrophotometer as described previously (*24*). HEPES buffer (100 mM) was used to maintain the pH at 7.4 and MES buffer (100 mM) at pH 5.6. Tiron (12 mM) served as the chelator at higher pH and EDTA (4 mM) at the lower pH. For Tiron, the absorbance maximum is located at 480 nm and increases as this chelator acquires the iron from hTF. For EDTA at pH 5.6, a decrease in absorbance at 293 nm allows observation of the disappearance of the iron-to-tyrosine charge-transfer band. Alternatively, since specifically bound iron in hTF quenches the intrinsic fluorescent signal, the release rate can also be monitored by following the increase in the fluorescence resulting from excitation at 280 nm and measurement of the emission signal at 330 nm. It is important to note that an identical rate of release from the C-lobe was obtained regardless of the method used to monitor the loss of iron. The kinetic data were fit to a single exponential decay function using Origin software (Version 7) to obtain a rate constant. All data reported are the result of at least three independent collections. The average rate is reported, and standard deviations from the mean are given.

Cell Binding Experiments. The protocols for preparing HeLa S_3 cells, conducting the competitive binding experiments, and analyzing the data have been previously reported (*21*, *25*). Briefly, diferric N-His hTF-NG was iodinated with $Na^{125}I$ by the method of McFarlane (*26*), yielding a preparation with a specific activity of 1.19×10^8 cpm/nmol. HeLa S_3 cells from three to five T-150 flasks were harvested,

Table 1: Production of Recombinant hTF Mutants

	maximum production (μg/mL) in				
mutant	N-His K206E hTF-NG		N-His Y95F/Y188F hTF-NG		
D392S	21.4 ± 2.1	$n = 2$	41.0 ± 3.7	$n = 2$	BA[a] +
Y426F	21.6 ± 7.7	$n = 3$	40.1 ± 9.8	$n = 2$	BA +
Y517F	24.9 ± 4.6	$n = 2$	38.3 ± 9.3	$n = 2$	BA +
H585A	21.6 ± 4.6	$n = 3$	59.5 ± 17.0	$n = 2$	BA +

[a] BA is butyric acid.

washed, and resuspended in 20 mM HEPES pH 7.4, containing 150 mM NaCl, 10 mM $NaHCO_3$, and 1% BSA. The cells were incubated for 15 min at 37 °C in the HEPES buffer also containing 20 mM NH_4Cl to inhibit the removal of iron. Cell suspensions (200 μL containing between 0.9 and 2.7×10^6 cells) were added to 12 × 75 mm plastic tubes containing a constant amount of diferric ^{125}I N-His hTF-NG (13.5 nM) and six different concentrations of unlabeled competitor in a total volume of 100 μL. For diferric competitors, final concentrations ranged from 20 to 400 nM; for monoferric and apo samples the range was 333−3333 nM. Following incubation for 30 min at 37 °C with shaking, the samples were processed by removal of duplicate 100 μL aliquots into Eppendorf tubes containing 800 μL of ice-cold HEPES buffer layered on 300 μL of dibutyl phthalate. The tubes were spun for 2 min in a Beckman microfuge B; the buffer and most of the dibutyl phthalate were aspirated, and the cell pellet was released by a hot wire into a 12 × 75 mm plastic tube for counting in a Packard γ counter. The data were processed as detailed previously (*25*).

RESULTS

Protein Production and Recovery. The amounts of recombinant hTF mutants produced by the BHK cells ranged between 20 and 60 mg/L of media at a maximum (Table 1). As recently documented, the addition of 1 mM butyric acid (BA) to the tissue culture medium in the roller bottles led to a significant increase in the expression of recombinant hTF (*22*). In the present work, this finding is further substantiated. The final recovery of recombinant hTF was between 50% and 60% of the amount measured by the immunoassay, which is also consistent with our recently reported results (*22*).

Spectral Analysis. The iron binding capability of hTF is reflected in its intrinsic spectral parameters. The absorbance maxima for the mutations in both the K206E and the Y95F/Y188F backgrounds are presented in Table 2. The wavelength of the visible absorbance maximum, A_{max}, and the ratio of A_{280}/A_{max} of the equivalent mutations in the N-lobe are also provided for comparison. Typical values for the ratio of A_{280}/A_{max} for diferric hTF are 20−25 and for monoferric hTF, ∼40. As recently noted, the visible absorbance maximum for the monoferric C-lobe is 461 vs 470 for the monoferric N-lobe which implies a subtle difference in the geometry of the binding site in the two lobes (*22*). Obviously, since all of the mutations in the K206E background have iron in the N-lobe, the absorbance maximum is the average of the contribution from each lobe. This somewhat masks the spectral properties and makes it more difficult to evaluate the direct effect of the mutations in the C-lobe. Therefore, each mutation was introduced into the hTF constructs with the Y95F/Y188F double mutation that prevents iron binding in the N-lobe (*22*). As observed with the N-lobe constructs, mutation of any of the liganding residues results in a significant blue shift in the absorbance maximum as most clearly observed for the constructs in the Y95F/Y188F background. In the case of both the D392S and H585A mutants, the visible maximum was so broad that it was not possible to determine the wavelength accurately. Additionally, the ratios of 24.1 and 26.2 for these mutants seem inconsistent with their classification as monoferric hTFs. The explanation appears to lie in the fact that the two Tyr ligands provide most of the visible signal which may be enhanced by the absence of either the D392 or H585 ligands. Unfortunately, the spectral data did not provide a convincing signature of iron binding for the Y426F mutant despite observation of a weak pinkish color in the sample. However, it was possible to conclude that the Y517F mutant did not bind iron in a specific manner since there was a complete absence of any color associated with the addition of iron to this mutant in the Y95F/Y188F construct.

Table 2: Spectral Data for Recombinant hTFs

N-His-tagged hTFs[a]	λ_{max}	A_{280}/A_{max}	ref
hTF	466	21.3	*20*
K206E hTF	463	25.6	*20*
Y95F/Y188F hTF (monoferric C-lobe)	461	42.2	*22*
K206E/**D392S** hTF	439	23.3	
Y95F/Y188F/**D392S** hTF	385−420	24.1	
D63S in N-lobe	426	22.8	*47*
K206E/**Y426F** hTF	444	33.5	
Y95F/Y188F/**Y426F** hTF	411	34.0	
Y95F in N-lobe	410	44.4	*10*
K206E/**Y517F** hTF	457	42.0	
Y95F/Y188F/**Y517F** hTF	no iron bound		
Y188F in N-lobe	no iron bound		*10*
K206E/**H585A** hTF	432	22.3	
Y95F/Y188F/**H585A** hTF	385−420	26.2	
H249A in N-lobe	439	23.8	*48*
Y426F/Y517F hTF (monoferric N-lobe)	470	41.4	*22*
Y95F/Y188F/**Y426F/Y517F** hTF (authentic apo)	no iron bound		*22*

[a] All hTF samples are His-tagged and nonglycosylated. Key mutations of the N- and C-lobes are indicated in bold.

EPR Spectra. The EPR data clearly show that diferric hTF-NG with or without the His tag has identical spectra with the classic three component $g' \sim 4.3$ signal that is a signature of specific iron binding (Figure 2, spectra a and b). In addition, the authentic apo-hTF (Y95F/Y188F/Y426F/Y517F) when presented with iron gives only a weak $g' = 4.3$ signal (spectrum f), corresponding to only ∼0.01 Fe(III)/protein such as is observed for adventiously bound iron. (Again the spectra are identical with and without the hexa-His tag.) The N-His Y95F/Y188F/D392S hTF-NG and N-His Y95F/Y188F/H585A hTF-NG give EPR spectra that are almost identical, consisting of sharp peak at $g' = 4.3$ with a slight shoulder to the low-field side (cf. spectra c and d). The double integrals of spectra c and d are approximately half that of spectrum a for the diferric protein, consistent with these mutants having one specifically bound iron, i.e., 1.07 ± 0.16 and 0.90 ± 0.14 Fe(III)/protein, respectively. The EPR spectrum e for the Y426F mutant when the protein is loaded with Fe(III) using Fe(II) and O_2 is weaker than those of either the D392S or the H585A mutants (spectra c and d). The corresponding Y426F double integral corre-

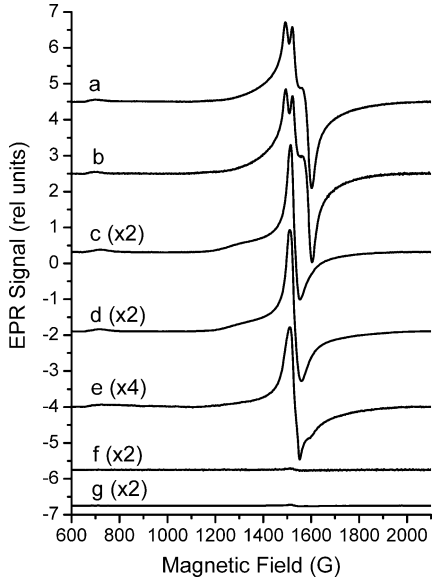

FIGURE 2: EPR spectra of recombinant hTFs and site-directed mutants: (a) diferric hTF-NG; (b) diferric N-His hTF-NG; (c) monoferric N-His Y95F/Y188F/D392S hTF-NG; (d) monoferric N-His Y95F/Y188F/H585A hTF-NG; (e) N-His Y95F/Y188F/Y426F hTF-NG plus 1 equiv of Fe(III); (f) apo N-His Y95F/Y188F/Y426F/Y517F hTF-NG plus 1 equiv of Fe(III); (g) N-His Y95F/Y188F/Y517F hTF-NG + 1 equiv of Fe(III). Conditions were 4 mg/mL protein in 0.1 M NH_4CO_3, pH 8.3, at 77 K. Spectrometer operating parameters are given in the Materials and Methods.

sponds to 0.27 ± 0.04 Fe(III)/protein in accord with the weaker binding in this mutant compared to D392S and H585A. When Fe(III)-NTA is employed to load the Y426F mutant, a composite EPR signal from a mixture of Fe(III)-NTA and another species, presumably protein-bound Fe(III), is observed (not shown), indicating that NTA competes with the protein for Fe(III). The very weak EPR signal (spectrum g) for the Y517F mutant in the Y95F/Y188F background corresponds to ~0.02 Fe(III)/protein and agrees with the other spectral data showing that this mutant lacks specific iron binding.

Iron Release at pH 7.4 and 5.6. As described above, only the D392S and H249A mutants bound iron with sufficient avidity and specificity to allow determination of iron release rates. The rate of iron release was measured for these mutants in both the K206E and Y95F/Y188F backgrounds at pH 7.4 and 5.6 and 25 °C (Table 3). It should be noted that, in the time frame of the studies described, iron release from the N-lobe of the K206E construct would be negligible (*20*). Conclusions from the iron release studies include the following: (1) At pH 7.4 the two mutants release iron considerably faster than the nonmutated C-lobe with the rate of release of the H585A mutant approximately 7-fold greater than found for the D392S. (2) At pH 7.4 the rate of release from the C-lobe is almost the same regardless of whether the N-lobe contains iron (K206E mutant) or not (Y95F/Y188F mutant) for each of the mutants. (3) In contrast, at pH 5.6 there is a difference in the rate of release from the K206E and Y95F/Y188F constructs. In the mutants, the N-lobe without iron (Y95F/Y188F) favors a somewhat faster release rate although the differences are not large (2-fold or less). It is important to remember that the actual rates of release at pH 7.4 and 5.6 cannot be compared directly due to differences in the experimental conditions. Therefore, the only legitimate comparison is to the nonmutated hTF control under each set of conditions.

Table 3: Iron Release Rates for the hTF C-Lobe

N-His-tagged protein	k_C (min^{-1})	n	k_C difference
(A) pH 7.4, 100 mM HEPES Buffer, 12 mM Tiron (Chelator), 25 °C			
hTF-NG	0.006 ± 0.001	5	1
K206E hTF-NG	0.007 ± 0.001	5	1.2
Y95F/Y188F/ hTF-NG	0.008 ± 0.0002	4	1.3
K206E/**D392S** hTF-NG	2.6 ± 0.2	6	430
Y95F/Y188F/**D392S** hTF-NG	2.1 ± 0.1	4	350
K206E/**H585A** hTF-NG	15.8 ± 1.1	5	2630
Y95F/Y188F/**H585A** hTF-NG	15.7 ± 0.8	5	2620
(B) pH 5.6, 100 mM MES Buffer, 4 mM EDTA (Chelator), 25 °C			
hTF-NG	0.021 ± 0.002	5	1.0
K206E hTF-NG	0.024 ± 0.001	5	1.1
Y95F/Y188F/ hTF-NG	0.025 ± 0.001	4	1.2
K206E/**D392S** hTF-NG	7.3 ± 0.4	7	350
Y95F/Y188F/**D392S** hTF-NG	11.6 ± 0.1	3	550
K206E/**H585A** hTF-NG	10.0 ± 0.3	5	480
Y95F/Y188F/**H585A** hTF-NG	18.1 ± 1.9	4	860

Table 4: Inhibition of Binding of Radioiodinated Diferric N-His hTF to HeLa S_3 Cell Receptors by Recombinant hTF Mutants[a]

protein	I_t[b] (nM)	R^2[c]	K_D (nM)	ratio[d]
Experiment A				
N-His hTF-NG (control)	30.0	0.994	5.4	1
N-His K206E hTF-NG (control)	31.5	0.994	5.9	1
N-His Y95F/Y188F hTF-NG (monoferric C-lobe)	580.1	0.998	237	42
N-His Y426F/Y517F hTF-NG (monoferric N-lobe)	528.4	0.991	215	38
Experiment B				
N-His hTF-NG (control)	33.8	0.993	10.4	1
N-His K206E/**Y426F** hTF-NG	80.6	0.997	34.5	3
N-His K206E/**H585A** hTF-NG	119.7	0.986	54.4	5
Experiment C				
N-His K206E hTF-NG (control)	24.6	0.998	6.6	1
N-His K206E/**D392S** hTF-NG	191.7	0.997	117	18
N-His K206E/**Y517F** hTF-NG	251.7	0.996	157	24
N-His Y426F/Y517F hTF-NG (monoferric N-lobe)	236.6	0.996	133	20

[a] Experiments A, B, and C were done on different days. [b] I_t is the total inhibitor concentration at 50% inhibition of ^{125}I Fe_2 N-His hTF-NG. [c] R^2 is the correlation coefficient for the straight line derived from plotting the log of the pmol/mL against log B/B_0. As described in Materials and Methods, I_t is found at log $B/B_0 = 0$. Note that the "authentic" apo sample N-His Y95F/Y188F/Y426F/Y517F hTF-NG did not inhibit binding at all. [d] The ratio is calculated by dividing the K_D of the mutants by the K_D of the control on a given day.

Cell Binding Experiments. Cell binding experiments were undertaken in an effort to determine whether the cleft in the C-lobe liganding mutants is in an open or closed conformation. We have found that the simplest and most reliable protocol for deriving an apparent K_D involves using a constant amount of radioiodinated hTF (in this study we used N-His hTF-NG) in competition with increasing concentrations of the various unlabeled hTF species. The amount of unlabeled competitor is selected to bracket the point at which 50% of the label is inhibited. The data shown in Table 4 are from experiments in which a reasonable range was obtained in each case. Due to the number of samples, multiple experiments were required. However, day-to-day reproducibility was reasonably good as demonstrated by the apparent K_D values for the control samples, which ranged from 5.4 to 10.4 nM for the three experiments shown in Table 4. The cell binding experiments clearly show that affinity is highest

Table 5: Comparison of Rate of Release for N-Lobe Liganding Mutants at 25 °C

protein	k_{Nobs} (min^{-1}) pH 7.4	pH 5.6
Y426F/Y517F hTF-N[a]	0.0229	6.3 ± 0.4, $n = 10$
hTF-NG[a]	0.0227	3.5 ± 0.1, $n = 5$
N-lobe hTF (hTF/2N)	0.0225[b]	9.5 ± 0.8, $n = 22$
D63S	153	3530/372[c]
Y95F	51.1	476
Y188F	no binding	no binding
H249A	295	3580

[a] These constructs contained an N-His tag. [b] Data for the N-lobe (except at pH 5.6) and all N-lobe mutants are from He and Mason (*7*). [c] Two rates were observed.

for the diferric controls, N-His hTF-NG and N-His K206E hTF-NG. The two monoferric samples, N-His Y95F/Y188F hTF-NG and N-His Y426F/Y517F hTF-NG, had lower affinities consistent with an apo N- or C-lobe, respectively. Interestingly, our authentic apo sample (N-His 95F/Y188F/Y426F/Y517F hTF-NG) showed no ability whatsoever to compete with the labeled diferric hTF for receptor binding under the stated conditions (and is thus not presented in Table 4). The N-His hTF-NG and N-His K206E hTF-NG constructs yield identical low K_D's as expected for diferric hTF. Additionally, hTF-NG with or without a His tag gave the equivalent binding constants of 9.1 and 10.8 nM when compared on the same day with the same batch of cells (data not shown). Also of interest, the ratios for the liganding mutants indicate that Y426F and H585A in the K206E background bind to cells with an affinity which is closer to that measured for the diferric samples than to that found for the monoferric controls. In contrast, the D392S and Y517F mutants in the K206E background bind with an affinity that is similar to that measured for the monoferric sample with the apo C-lobe.

Of special note is that the calculated K_D values for the two authentic monoferric proteins (N-His Y95F/Y188F hTF-NG and N-His Y426F/Y517F hTF-NG) are indistinguishable, with a binding affinity that is ~40-fold lower than the diferric control, regardless of which lobe contains the iron. A previous study reported that the standard free energy of binding of the isolated C-lobe to the TFR was −32.4 kJ as calculated from $\Delta G = -RT \ln K_A$, where K_A is the association constant for the interaction. Thus the C-lobe alone appeared to provide the majority (76%) of the binding energy (*12*). Those experiments were performed at 4 °C and measured transferrin binding to TFR on K562 cells. Calculation of the free energy of binding of the two monoferric hTFs compared to diferric hTF in our HeLa S_3 experiments (pretreated to prevent iron removal) at 37 °C yields estimates of −48.1 ± 2.0 kJ ($n = 8$) for diferric hTF, −39.6 ± 0.3 kJ ($n = 3$) for N-His Y95F/Y188F hTF-NG (monoferric C-lobe), and −39.9 ±0.8 kJ ($n = 3$) for N-His N-His Y426F/Y517F hTF-NG (monoferric N-lobe). Thus, the two monoferric hTFs have an essentially equivalent free energy of binding, which in each case is 82% of that of diferric hTF.

Comparison to the N-Lobe. As shown in Table 5, at pH 7.4 and 25 °C, the rate of iron release measured for the N-lobe is virtually identical whether the C-lobe has iron (hTF-NG), is unoccupied (N-His Y426F/Y517F hTF-NG), or is absent (hTF/2N). However, at pH 5.6 and 25 °C, differences in the rate of release between the various samples are apparent. The release rate from the N-lobe when iron is present in the C-lobe is 3.5 min^{-1} compared to 6.3 min^{-1} when the C-lobe lacks iron and 9.5 min^{-1} when the C-lobe is absent (in hTF/2N). Although previously the rate from the recombinant N-lobe was reported as 4.99 min^{-1} (*7*), more recently we have consistently obtained a rate of 9.5 min^{-1} using a temperature-controlled spectrophotometer. The previous kinetic runs were conducted at "room temperature" whereas a thermostated Peltier accessory (CARY-100) or a circulating water bath (Olis) has been used in the more recent experiments.

DISCUSSION

The binding of hTF to its specific receptor is based on molecular recognition which is complicated by the bilobal nature of hTF and the large and dynamic conformational changes in each lobe that accompany iron binding and release. In fact, it has been suggested that the bilobal structure may provide additional levels of control (*2*). The role of the receptor (*27*), of lobe−lobe interaction (*13*, *25*, *28*−*37*), and of the orientation and flexibility of the lobes (*2*, *38*) have all been areas of active research. It is clear that the receptor discriminates between the various forms of hTF in a pH-sensitive manner and is an active participant in the mechanism of iron release. The net result is that iron is released at the proper time and in the appropriate environment for transport out of the endosome. Thus the binding of hTF to receptor slows iron release from each lobe at pH 7.4 and accelerates it at pH 5.6, the approximate pH of the endosome. As described in more detail below, this is especially important in the case of the C-lobe, which has an inherently slower rate of iron release.

In the current study, the effect of mutating the C-lobe liganding residues on the iron binding and release properties of the holoprotein was evaluated. First, it was critical to determine whether each of the mutants retained the ability to bind iron in the C-lobe; this challenge proved more difficult than anticipated. In previous work with the recombinant N-lobe, EPR spectra provided the definitive proof that the Y188F mutant was unable to bind iron (*10*). Similarly, in the current work EPR studies revealed a complete absence of specific iron binding in the Y517F mutant (Figure 2, spectrum g), supporting the conclusions from the UV−vis spectral data (Table 2). In the case of the Y426F mutant, the EPR signal was suggestive of formation of a comparatively weak iron complex (Figure 2, spectrum e). Additionally, the UV−vis spectrum did not have an easily discernible absorption band associated with specific iron binding although a faint pink color was noted. We conclude that the binding of iron to this mutant is extremely weak. This is in contrast to the equivalent tyrosine mutant in the N-lobe (Y95F), which gave a clear visible spectrum, a convincing EPR signal indicative of specific iron binding, and from which we were able to determine iron release rates (*10*). Thus, in the C-lobe both tyrosine ligands are essential to specific iron binding whereas in the N-lobe only the Y188 ligand is critical (a finding that is perhaps indicative of less flexibility in the C-lobe).

Since the D392S and H585A mutants yielded similar EPR spectra (Figure 2, spectra c and d), it seemed possible each

might have the same ligand set, consisting simply of the two Tyr ligands (Y426 and Y517) and the synergistic carbonate anion. Support for this idea comes from the UV−vis spectra for these two mutants in the Y95F/Y188F background, which give a stronger than expected broad visible signal and a similar A_{280}/A_{max} ratio (Table 2). The loss of coordination of Asp392 also implies that the binding cleft is open (*39*) and that the lack of binding to Asp392 might preclude iron binding to His585 and vice versa. Since the coordinate-covalent bonds to the iron comprise the main force holding the domains together (*38*), mutation of any of the liganding residues would favor domain opening.

Because it has been well established that the specific hTF receptor distinguishes between diferric, monoferric, and apo-TF (*5*, *25*, *40*), cell binding experiments were conducted to determine the binding affinities of each C-lobe ligand mutant in monoferric hTF constructs (N-His K206E hTF-NG) to try to assess the conformation of the C-lobe (open or closed). As shown in Table 4, the data are consistent with the conclusion that the D392S and Y517F mutants are in an open conformation since the K_D values are 18- and 24-fold higher than the diferric control, respectively. In this case we considered that the Y517F mutant might serve as a positive control since the complete inability to bind iron is presumed to favor the open conformation. This interpretation is reinforced by the fact that our authentic recombinant apo-hTF (with no ability to bind iron in either lobe) did not inhibit binding of the labeled diferric hTF at all, implying that both lobes were in the open conformation. Somewhat surprisingly, the K_D values for the Y426F and H585A mutations are indicative of a cleft which is nearly closed (with ratios of 3 and 5, respectively). Obviously, the binding constants that are measured reflect the equilibrium state with participation of the TFR. Of possible relevance is that Y426 and H585 both reside in the hinge region. Clearly, the equilibrium conditions favor the closed conformation for these two mutants (see below).

A significant finding from the equilibrium binding experiments is that the free energy of diferric hTF binding to receptor is not simply the sum of the free energies of the individual monoferric proteins but significantly less. The free energy of diferric hTF binding is −48.1 kJ/mol, whereas each of the two monoferric species have free energies of binding of (−39.6) + (−39.9) = −79.5 kJ/mol. Thus, each monoferric species contributes almost equally to the binding energy at a level that is 82% of the diferric hTF. In the studies in which the isolated C-lobe was shown to account for 76% of the binding energy, it was naturally assumed that the sum of the free energies would be equal to the diferric species (*12*). Our results therefore support a nearly equivalent role for both the iron-containing N-lobe and C-lobes in binding to the TFR, consistent with our previous work (*11*, *34*) as well as other studies (*6*). The recently published EM model of the hTF/TFR complex (*41*) indicates that contact with the helical region of the TFR resides in 11 residues in the C-I domain (between positions 349 and 372) and involves ionic interactions, apparently leaving the C-II domain free to swing open. In the same model, contact with the N-lobe is more localized though it does appear to involve the N-I and N-II domains interacting with both the helical and protease-like domains of the TFR. Additionally, the model predicts a 9 Å movement of the N-lobe with respect to the C-lobe to accommodate receptor binding. Many features of the model are supported by the extensive TFR mutagenesis studies of Giannetti et al. (*42*). However, future models must account for the significant contribution to the binding energy of the iron-containing N-lobe (in the monoferric construct). As suggested (*27*), the "stalk" connecting the TFR to the transmembrane region of the receptor (and absent in the soluble recombinant TFR) could participate in binding to the N-lobe. The TFR in our cell binding experiments retains this stalk region, which could provide some of the binding energy.

Comparison of the rate constants for the two lobes shows that under the identical conditions the rate of iron release from the C-lobe at pH 7.4 (N-His Y95F/Y188F hTF-NG) is approximately 4-fold slower than the rate for the N-lobe in the N-His Y426F/Y517F hTF-NG construct (0.008 vs 0.0229 min^{-1}). At this pH, the effect of mutations to the liganding residues in the N-lobe has a profound effect on the rate of iron release (Table 5). For the two mutants that can be directly compared, the D63S and the H249A substitutions increase the rate of release 6800- and 13000-fold, respectively, compared to the unmutated N-lobe. The effect of introducing the same mutations (D392S and H585A) into the C-lobe results in more modest 400- and 2500-fold increases, an entire order of magnitude lower (Table 3A). These differences cannot be accounted for by the inherent difference in the release rate of each lobe that, as noted above, is approximately 4-fold.

At pH 5.6, the effect of singly mutating the Asp or His ligand in the N-lobe leads to an ∼400-fold faster release rate compared to nonmutated N-lobe (Tables 3 and 5). A similar 300−400-fold enhancement in rates is observed for the corresponding mutations in the C-lobe. However, in every instance, the C-lobe and the C-lobe mutants when compared to the N-lobe and its mutants release iron at rates that are at least 200-fold slower (cf. Tables 3 and 5). Thus, the data from these kinetic studies highlight the role of the TFR in accelerating the release of iron from the C-lobe in cells (*6*, *43*), a process that is otherwise predicted to be slow based on the in vitro kinetics reported here in Tables 3 and 5.

The N- and C-lobes of hTF differ in a number of aspects. The C-lobe of hTF contains 11 disulfide bonds, whereas the N-lobe has only 8 (*44*). The C-lobe has a triad of residues (Lys534-Arg632-Asp634) that definitely play a role in the release of iron (*20*, *45*), whereas the N-lobe has a dilysine pair (Lys206 and Lys296) that is important in the process (*45*, *46*). The C-lobe features a 9 nm blue shift in the visible absorbance maximum relative to the diferric protein, a finding indicative of a subtle difference in the C-lobe coordination sphere of constructs lacking iron in the N-lobe (*22*). Lastly, the addition of salt leads to a significant increase in the rate of iron release from the C-lobe at all pH values (*20*) whereas in the N-lobe the presence of salt actually slows iron release at pH 7.4 and increases it at pH 5.6 (*7*).

The current work utilizes our recently developed mutational strategy to completely control the iron status of the N-lobe, allowing determination of kinetic rate constants for the C-lobe and two of the C-lobe liganding mutants. Comparison of these rates to the rates of the same mutants in the N-lobe substantiate and extend the well-known differences between the two lobes. The measured dissociation constants for the binding of authentic monoferric transferrins to the receptor indicate that the strengths of binding attributed

to the individual N- and C-lobes are the same within experimental error and document the importance of lobe−lobe (negative) cooperativity in the overall strength of binding which is less than the sum of the individual lobes. Additionally, the receptor binding studies on the C-lobe mutants predict the conformational state of the C-lobe in each during binding.

REFERENCES

1. Aisen, P., Enns, C., and Wessling-Resnick, M. (2001) Chemistry and biology of eukaryotic iron metabolism, *Int. J. Biochem. Cell Biol. 33*, 940−959.
2. Baker, E. N., Baker, H. M., and Kidd, R. D. (2002) Lactoferrin and transferrin: Functional variations on a common structural framework, *Biochem. Cell Biol. 80*, 27−34.
3. Zuccola, H. J. (1993) The crystal structure of monoferric human serum transferrin, Ph.D. Thesis, Georgia Institute of Technology, Atlanta, GA.
4. Hall, D. R., Hadden, J. M., Leonard, G. A., Bailey, S., Neu, M., Winn, M., and Lindley, P. F. (2002) The crystal and molecular structures of diferric porcine and rabbit serum transferrins at resolutions of 2.15 and 2.60 Å, respectively, *Acta Crystallogr., Sect. D: Biol. Crystallogr. 58*, 70−80.
5. Klausner, R. D., Ashwell, G., van Renswoude, J., Harford, J. B., and Bridges, K. R. (1983) Binding of apotransferrin to K562 cells: Explanation of the transferrin cycle, *Proc. Natl. Acad. Sci. U.S.A. 80*, 2263−2266.
6. Zak, O., and Aisen, P. (2003) Iron release from transferrin, its C-lobe, and their complexes with transferrin receptor: Presence of N-lobe accelerates release from C-lobe at endosomal pH, *Biochemistry 42*, 12330−12334.
7. He, Q.-Y., and Mason, A. B. (2002) Molecular aspects of release of iron from transferrins, in *Molecular and Cellular Iron Transport* (Templeton, D. M., Ed.) pp 95−123, Marcel Dekker, New York.
8. Jeffrey, P. D., Bewley, M. C., MacGillivray, R. T. A., Mason, A. B., Woodworth, R. C., and Baker, E. N. (1998) Ligand-induced conformational change in transferrins: crystal structure of the open form of the N-terminal half-molecule of human transferrin, *Biochemistry 37*, 13978−13986.
9. MacGillivray, R. T. A., Moore, S. A., Chen, J., Anderson, B. F., Baker, H., Luo, Y. G., Bewley, M., Smith, C. A., Murphy, M. E., Wang, Y., Mason, A. B., Woodworth, R. C., Brayer, G. D., and Baker, E. N. (1998) Two high-resolution crystal structures of the recombinant N-lobe of human transferrin reveal a structural change implicated in iron release, *Biochemistry 37*, 7919−7928.
10. He, Q.-Y., Mason, A. B., Woodworth, R. C., Tam, B. M., MacGillivray, R. T. A., Grady, J. K., and Chasteen, N. D. (1997) Inequivalence of the two tyrosine ligands in the N-lobe of human serum transferrin, *Biochemistry 36*, 14853−14860.
11. Mason, A. B., Tam, B. M., Woodworth, R. C., Oliver, R. W. A., Green, B. N., Lin, L.-N., Brandts, J. F., Savage, K. J., Lineback, J. A., and MacGillivray, R. T. A. (1997) Receptor recognition sites reside in both lobes of human serum transferrin, *Biochem. J. 326*, 77−85.
12. Zak, O., and Aisen, P. (2002) A new method for obtaining human transferrin C-lobe in the native conformation: Preparation and properties, *Biochemistry 41*, 1647−1653.
13. Mason, A. B., He, Q. Y., Halbrooks, P. J., Everse, S. J., Gumerov, D. R., Kaltashov, I. A., Smith, V. C., Hewitt, J., and MacGillivray, R. T. A. (2002) Differential effect of a His tag at the N- and C-termini: Functional studies with recombinant human serum transferrin, *Biochemistry 41*, 9448−9454.
14. Gumerov, D. R., Mason, A. B., and Kaltashov, I. A. (2003) Interlobe communication in human serum transferrin: Metal binding and conformational dynamics investigated by electrospray ionization mass spectrometry, *Biochemistry 42*, 5421−5428.
15. Princiotto, J. V., and Zapolski, E. J. (1975) Difference between the two iron-binding sites of transferrin, *J. Biol. Chem. 253*, 1930−1937.
16. Cannon, J. C., and Chasteen, N. D. (1975) Nonequivalence of the metal binding sites in vanadyl-labeled human serum transferrin, *Biochemistry 14*, 4573−4577.
17. Lestas, A. N. (1976) The effect of pH upon human transferrin: selective labelling of the two iron-binding sites, *Br. J. Haematol. 32*, 341−350.
18. Baldwin, D. A., and DeSousa, D. M. R. (1981) The effect of salts on the kinetics of iron release from N-terminal and C-terminal monoferric transferrins, *Biochem. Biophys. Res. Commun. 99*, 1101−1107.
19. Marques, H. M., Watson, D. L., and Egan, T. J. (1991) Kinetics of iron removal from human serum monoferric transferrins by citrate, *Inorg. Chem. 30*, 3758−3762.
20. Halbrooks, P. J., He, Q. Y., Briggs, S. K., Everse, S. J., Smith, V. C., MacGillivray, R. T. A., and Mason, A. B. (2003) Investigation of the mechanism of iron release from the C-lobe of human serum transferrin: Mutational analysis of the role of a pH sensitive triad, *Biochemistry 42*, 3701−3707.
21. Mason, A. B., Miller, M. K., Funk, W. D., Banfield, D. K., Savage, K. J., Oliver, R. W. A., Green, B. N., MacGillivray, R. T. A., and Woodworth, R. C. (1993) Expression of glycosylated and nonglycosylated human transferrin in mammalian cells. Characterization of the recombinant proteins with comparison to three commercially available transferrins, *Biochemistry 32*, 5472−5479.
22. Mason, A. B., Halbrooks, P. J., Larouche, J. R., Briggs, S. K., Moffett, M. L., Ramsey, J. E., Connolly, S. A., Smith, V. C., and MacGillivray, R. T. A. (2004) Expression, purification, and characterization of authentic monoferric and apo-human serum transferrins, *Protein Expression Purif. 36*, 318−326.
23. Mason, A. B., He, Q.-Y., Adams, T. E., Gumerov, D. R., Kaltashov, I. A., Nguyen, V., and MacGillivray, R. T. A. (2001) Expression, purification, and characterization of recombinant nonglycosylated human serum transferrin containing a C-terminal hexahistidine tag, *Protein Expression Purif. 23*, 142−150.
24. He, Q. Y., Mason, A. B., Nguyen, V., MacGillivray, R. T. A., and Woodworth, R. C. (2000) The chloride effect is related to anion binding in determining the rate of iron release from the human transferrin N-lobe, *Biochem. J. 350*, 909−915.
25. Mason, A. B., He, Q.-Y., Tam, B. M., MacGillivray, R. T. A., and Woodworth, R. C. (1998) Mutagenesis of the aspartic acid ligands in human serum transferrin: lobe-lobe interaction and conformation as revealed by antibody, receptor-binding and iron-release studies, *Biochem. J. 330*, 35−40.
26. McFarlane, A. S. (1963) In vivo behavior of I131-fibrinogen, *J. Clin. Invest. 42*, 346−361.
27. Aisen, P. (2004) Transferrin receptor 1, *Int. J. Biochem. Cell Biol. 36*, 2137−2143.
28. Bali, P. K., and Harris, W. R. (1989) Cooperativity and heterogeneity between the two binding sites of diferric transferrin during iron removal by pyrophosphate, *J. Am. Chem. Soc. 111*, 4457−4461.
29. Bali, P. K., Harris, W. R., and Nesset-Tollefson, D. (1991) Kinetics of iron removal from monoferric and cobalt-labeled monoferric human serum transferrin by nitrilotris(methylenephosphonic acid) and nitrilotriacetic acid, *Inorg. Chem. 30*, 502−508.
30. Beatty, E. J., Cox, M. C., Frenkiel, T. A., Tam, B. M., Mason, A. B., MacGillivray, R. T. A., Sadler, P. J., and Woodworth, R. C. (1996) Interlobe communication in ^{13}C-methionine-labeled human transferrin, *Biochemistry 35*, 7635−7642.
31. Lin, L.-N., Mason, A. B., Woodworth, R. C., and Brandts, J. F. (1994) Calorimetric studies of serum transferrin and ovotransferrin. Estimates of domain interactions, and study of the kinetic complexities of ferric ion binding, *Biochemistry 33*, 1881−1888.
32. Kurokawa, H., Mikami, B., and Hirose, M. (1994) Crucial role of intralobe peptide-peptide interactions in the uptake and release of iron by ovotransferrin, *J. Biol. Chem. 269*, 6671−6676.
33. Lin, L., Mason, A. B., Woodworth, R. C., and Brandts, J. F. (1991) Calorimetric studies of the binding of ferric ions to ovotransferrin and interactions between binding sites, *Biochemistry 30*, 11660−11669.
34. Mason, A. B., Woodworth, R. C., Oliver, R. W. A., Green, B. N., Lin, L.-N., Brandts, J. F., Savage, K. J., Tam, B. M., and MacGillivray, R. T. A. (1996) Association of the two lobes of ovotransferrin is a prerequisite for receptor recognition. Studies with recombinant ovotransferrins., *Biochem. J. 319*, 361−368.
35. Okamoto, I., Mizutani, K., and Hirose, M. (2004) Iron-binding process in the amino- and carboxyl-terminal lobes of ovotransferrin: Quantitative studies utilizing single Fe^{3+}-binding mutants, *Biochemistry 43*, 11118−11125.
36. Day, C. L., Stowell, K. M., Baker, E. N., and Tweedie, J. W. (1992) Studies of the N-terminal half of human lactoferrin produced from the cloned cDNA demonstrate that interlobe interactions modulate iron release, *J. Biol. Chem. 267*, 13857−13862.

37. Ward, P. P., Zhou, X., and Conneely, O. M. (1996) Cooperative interactions between the amino- and carboxyl-terminal lobes contribute to the unique iron-binding stability of lactoferrin, *J. Biol. Chem. 271*, 12790−12794.
38. Baker, H. M., Anderson, B. F., and Baker, E. N. (2003) Dealing with iron: Common structural principles in proteins that transport iron and heme, *Proc. Natl. Acad. Sci. U.S.A. 100*, 3579−3583.
39. Grossmann, J. G., Mason, A. B., Woodworth, R. C., Neu, M., Lindley, P. F., and Hasnain, S. S. (1993) Asp ligand provides the trigger for closure of transferrin molecules. Direct evidence from X-ray scattering studies of site-specific mutants of the N-terminal half-molecule of human transferrin, *J. Mol. Biol. 231*, 554−558.
40. Young, S. P., Bomford, A., and Williams, R. (1984) The effect of the iron saturation of transferrin on its binding and uptake by rabbit reticulocytes, *Biochem. J. 219*, 505−510.
41. Cheng, Y., Zak, O., Aisen, P., Harrison, S. C., and Walz, T. (2004) Structure of the human transferrin receptor-transferrin complex, *Cell 116*, 565−576.
42. Giannetti, A. M., Snow, P. M., Zak, O., and Bjorkman, P. J. (2003) Mechanism for multiple ligand recognition by the human transferrin receptor, *PLoS Biol. 1*, 341−350.
43. Bali, P. K., Zak, O., and Aisen, P. (1991) A new role for the transferrin receptor in the release of iron from transferrin, *Biochemistry 30*, 324−328.
44. Spik, G., Coddeville, B., and Montreuil, J. (1988) Comparative study of the primary structures of sero-, lacto- and ovotransferrin glycans from different species, *Biochimie 70*, 1459−1469.
45. Dewan, J. C., Mikami, B., Hirose, M., and Sacchettini, J. C. (1993) Structural evidence for a pH-sensitive dilysine trigger in the hen ovotransferrin N-lobe: Implications for transferrin iron release, *Biochemistry 32*, 11963−11968.
46. He, Q.-Y., Mason, A. B., Tam, B. M., MacGillivray, R. T. A., and Woodworth, R. C. (1999) Dual role of Lys206-Lys296 interaction in human transferrin N-lobe: Iron-release trigger and anion-binding site, *Biochemistry 38*, 9704−9711.
47. Woodworth, R. C., Mason, A. B., Funk, W. D., and MacGillivray, R. T. A. (1991) Expression and initial characterization of five site-directed mutants of the N-Terminal half-molecule of human transferrin, *Biochemistry 30*, 10824−10829.
48. He, Q.-Y., Mason, A. B., Pakdaman, R., Chasteen, N. D., Dixon, B. L., Tam, B. M., Nguyen, V., MacGillivray, R. T. A., and Woodworth, R. C. (2000) Mutations at the histidine 249 ligand profoundly alter the spectral and iron-binding properties of human serum transferrin N-lobe, *Biochemistry 39*, 1205−1210.
49. DeLano, W. L. (2002) The PyMOL Molecular Graphics System (http://www.pymol.org).

BI050015F